Stark control of electrons across interfaces

Antonio J. Garzón-Ramírez and Ignacio Franco

Phys. Rev. B **98**, 121305 — Published 24 September 2018

DOI: 10.1103/PhysRevB.98.121305

Stark Control of Electrons Across Interfaces

Antonio J. Garzón-Ramírez[1] and Ignacio Franco[1,2]

[1]*Department of Chemistry, University of Rochester, Rochester, New York 14627, USA*
[2]*Department of Physics, University of Rochester, Rochester, New York 14627, USA**

(Dated: September 5, 2018)

We introduce a laser control scenario to transiently transform an insulating heterojunction into a conducting one on a femtosecond timescale. The scenario is based on opening Landau-Zener quantum tunneling channels for electron transfer between two adjacent semiconductors via Stark shifts induced by non-resonant lasers of intermediate intensity (non-perturbative but non-ionizing). Through quantum dynamics simulations we demonstrate the robustness of the approach and its utility for controlling electron dynamics at interfaces.

A general goal in our quest to control matter and energy is the design of laser control strategies[1–4] to manipulate electronic properties and electron dynamics. In addition to its interest at the fundamental level, lasers permit ultrafast manipulation[5–11] opening new ways to design electronics and photoelectronic actuators that operate in a femto to attosecond timescale.

In this Letter, we propose a laser control scenario to transiently turn a perfect composite insulator into a conducting one on a femtosecond timescale. The scenario is based on using Stark shifts induced by non-resonant light of intermediate intensity (non-perturbative but non-ionizing) to open quantum tunneling pathways for electron transfer between two adjacent semiconductors. Below, the scenario is demonstrated by solving the time-dependent Schrödinger equation for a model tight-binding heterojunction, and explained through Landau-Zener tunneling theory. These results demonstrate a general route for control of electron dynamics at interfaces, and illustrate the power of Stark based strategies for control of matter[9,11–14].

Control through the Stark effect is a form of Hamiltonian control, based on shifting energy levels through non-resonant light[11–13,15–18]. As a mechanism of laser control of electrons it has the advantage of being robust to decoherence[11,19] because it does not exploit the fragile coherence properties of electronic superposition states. This feature is crucial as electronic decoherence in matter is remarkably fast[20–23], making traditional coherent control schemes based on interference effects to be of limited applicability[19]. While Stark control of electron dynamics at the metal-dielectric interface has been recently demonstrated[9,11,14], Stark schemes across the semiconductor-semiconductor interface represents an unexplored frontier in the laser control of electron dynamics.

The use of light to modify the electronic properties of bulk materials is a subject of considerable current interest. Recent progress includes schemes to create light-induced dynamical gaps[24–27] that modify the transport properties[28], and scenarios to modify the optical properties[10,29]. The scheme proposed here differs from these previous efforts in that it focuses on the effect of light on the effective interfacial coupling between materials.

As a model system we consider a heterojunction composed of two adjacent one-dimensional two-band tight-binding semiconductors (Fig. 1a), and focus on the exemplifying case in which the two materials have no spectral overlap, the interface is atomically sharp and band bending does not play a role (Model 1 in Fig. 2a). This guarantees that the heterojunction behaves as a perfect insulator to an applied voltage or to resonant photoexcitation as there is no path for exchange of electrons between the two materials. However, the identified scheme is general and can apply to more complex interfaces.

The basic concept behind the proposed scenario is illustrated in Fig. 1. Through Stark effects, the electric field of light distorts the electronic structure of the heterojunction (Fig. 1b). This deformation leads to transient resonances between electronic eigenstates of material A and B. When a valence band (VB) eigenstate of one material (say A) enters into transient resonance with a conduction band (CB) eigenstate of the other material (B), A→B tunneling electron transfer across the heterojunction occurs. These quantum tunneling pathways for electron transfer are particularly effective when the eigenstates involved are both localized at the interface (Fig. 1d), leading to a significant avoided crossing in the energy level diagram as a function of increasing electric field (Fig. 1c).

To demonstrate this concept, we solve the time-dependent Schrödinger equation for a model heterojunction in the presence of few cycle non-resonant light. The model Hamiltonian is given by

$$\hat{H} = \hat{H}_{\rm A} + \hat{H}_{\rm B} + \hat{H}_{\rm AB}, \tag{1}$$

where $\hat{H}_i$ is the Hamiltonian for material i = A or B, and $\hat{H}_{\rm AB}$ the interfacial coupling between the semiconductors. Each material is modeled as a two-band tight-binding chain with $N_i = 50$ unit cells (100 sites) in dipole interaction with a laser field $E(t)$

$$\hat{H}_i = \sum_{n=1}^{2N_i} (h^i_{nn} + |e|E(t)x_n)\hat{a}^\dagger_n \hat{a}_n + \sum_{\langle n,m\rangle}^{2N_i} h^i_{nm}(\hat{a}^\dagger_n \hat{a}_m + \text{h.c.}), \tag{2}$$

where $\langle n,m\rangle$ denotes nearest-neighbors, and h.c. hermitian conjugate. Here $\hat{a}_n$ ($\hat{a}^\dagger_n$) annihilates (creates) a fermion in site n and satisfies the usual fermionic

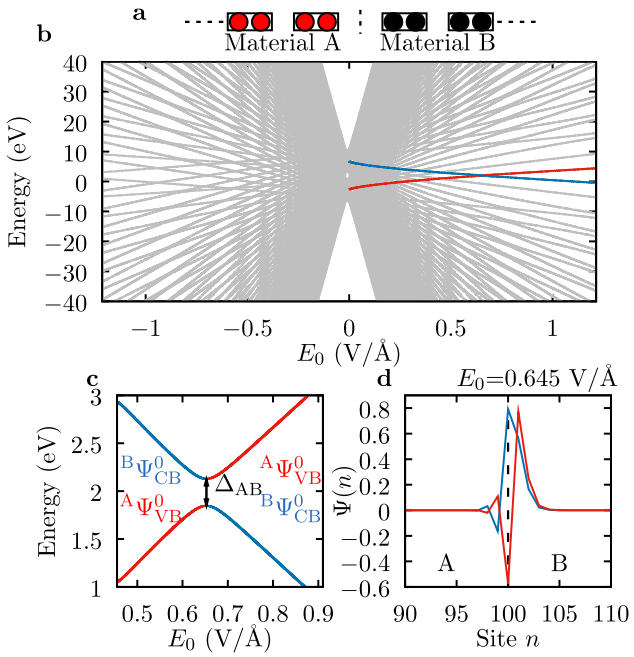

FIG. 1. Laser-induced electron tunneling across interfaces through Stark shifts. (**a**) Scheme of a heterojunction composed of two adjacent two-band semiconducting materials A and B. Under the influence of a non-resonant laser field, (**b**) the laser-dressed eigenenergies of the heterojunction (obtained by diagonalizing $\hat{H}$ [Eq. (1)] for a fixed electric field E_0) fan out as the laser field amplitude E_0 increases resulting in multiple trivial and avoided crossings. Avoided crossings between levels that belong to different materials, such as that signaled by the colored lines in (**b**) and detailed in (**c**), open tunneling pathways for electron transfer. The crossing in (**c**) is between a VB level of A (with eigenfunction $^{A}\Psi^0_{VB}$) and a CB level of B ($^{B}\Psi^0_{CB}$). These crossing are particularly effective when the wave functions of the dressed states spatially overlap at the interface (n =100-101, in this case) as in (**d**) leading to significant energy gap Δ_{AB} at the avoided crossing.

anticommutation relations. Each unit cell has two Wannier functions with alternating on-site energies ($h^i_{nn} = h^i_{\rm even}\delta_{n,\rm even} + h^i_{\rm odd}\delta_{n,\rm odd}$), in tight-binding coupling among them ($h^i_{n,n+1} = t^i_{\rm even}\delta_{n,\rm even} + t^i_{\rm odd}\delta_{n,\rm odd}$). Here x_n denotes the position of each Wannier function along the junction, and $|e|$ the electron charge. The interaction between the semiconductors at the interface is given by $\hat{H}_{\rm AB} = -t_{\rm AB}(\hat{a}^\dagger_{2N_A}\hat{a}_{2N_A+1} + \text{h.c.})$, where $t_{\rm AB}$ is the interfacial tight-binding coupling. For definiteness, we choose a lattice constant of $a = 5.0$ Å and a distance between sites in each cell of 1.7 Å in both materials. The interfacial distance is $a_{\rm AB}$ =7.7 Å and $t_{\rm AB}$ =0.2 eV. The remaining tight-binding parameters are defined in Fig. 2.

The vector potential associated with the electric field $E(t) = -\dot{A}(t)$ of amplitude E_0 employed in the simulations is of the form $A(t) = \frac{E_0}{\omega}e^{-(t-t_c)^2/2\tau^2}\sin(\omega(t-t_c)+\phi)$. This form guarantees that $E(t)$ is an ac-source as $\int_{-\infty}^{\infty}E(t)dt = A(-\infty) - A(\infty) = 0$. In the simulations, we employ few cycle lasers of central frequency $\hbar\omega$ =0.5 eV, carrier envelope phase $\phi = 0$, width τ =5.85 fs, centered around t_c =50 fs (see Fig. 2). A few-cycle laser is chosen to suppress the onset of dielectric breakdown[10,30,31] even for moderately strong fields. In turn, the frequency is chosen to be far detuned from any electronic transition such that Stark effects, and not near-resonance photon absorption, dominate the dynamics.

Since the Hamiltonian of Eq. (1) is a single particle operator, the electronic properties of this system are completely characterized by the electronic reduced density matrix $\rho_{nm}(t) = \langle\psi(t)|\,\hat{a}^\dagger_n\hat{a}_m\,|\psi(t)\rangle$, where $|\psi(t)\rangle$ is the many-body wavefunction. The dynamics of ρ_{nm} is determined by $i\hbar\frac{d}{dt}\rho_{nm}(t) = \left\langle\left[\hat{a}^\dagger_n\hat{a}_m, \hat{H}\right]\right\rangle$, with initial condition $\rho_{nm}(0) = \sum^N_\varepsilon\langle\varepsilon|n\rangle\langle m|\varepsilon\rangle f(\varepsilon)$. Here $|\varepsilon\rangle$ are the single particle eigenstates of $\hat{H}$ at $t = 0$, and $f(\varepsilon)$ the initial distribution function that takes values of 0 or 1 depending of the initial occupation of each $|\varepsilon\rangle$. These equations are numerically integrated using the Adams-Moulton method[32].

Figure 2c shows the charge transfer dynamics induced by a few-cycle laser pulse (upper panel) across the insulating heterojunction (Model 1, Fig. 2a). The amount of charge that is transferred from material A to B at time t is quantified by $Q_{\rm A\to B}(t) = -|e|\sum_{n=1}^{N_A}\int_0^t dt'(\rho_{nn}(t') - \rho_{nn}(0))$. As shown, once the laser amplitude reaches certain threshold intensity population is transferred from A to B. At that intensity the Stark shifts induced by the laser generate transient resonances between VB eigenstates of material A and the CB eigenstates of material B. Therefore, quantum tunneling channels are opened between A and B allowing for electrons flux from A to B, and turning this insulating heterojunction into a transient conductor on a femtosecond timescale.

Figure 2d shows the net charge transferred $Q_{\rm A\to B}(\infty)$ by laser pulses of varying amplitude. We observe three regions in the response. In region I ($E_0 \le 0.076$ V/Å) while the laser induces several crossings these transient resonances are between levels that have no significant spatial overlap and, thus, do not lead to appreciable charge transfer. In region II ($0.076 < E_0 \lesssim 0.5$ V/Å, intensity $7.7\times10^{10} < I_0 \lesssim 3.3\times10^{12}$ W/cm^2), the transient resonances that lead to charge transfer are mainly due to avoided crossings between levels in the VB of A and the CB of B. As the laser amplitude increases, more crossing between levels with significant spatial overlap occur leading to an increase in the transferred charge. Figure 1c details the most effective of these crossings, which is between the lowest energy level of the VB of A and the highest energy level of the CB of B. Notice that due to the localization of the energy levels by the interaction with the laser pulse, the wavefunctions overlap at the interface (see Fig. 1d). In region III ($E_0 \gtrsim 0.5$ V/Å), the laser is intense enough to induce crossings between the VB of B and the CB of A that lead to B→A charge transfer and large Zener interband tunneling[33] in

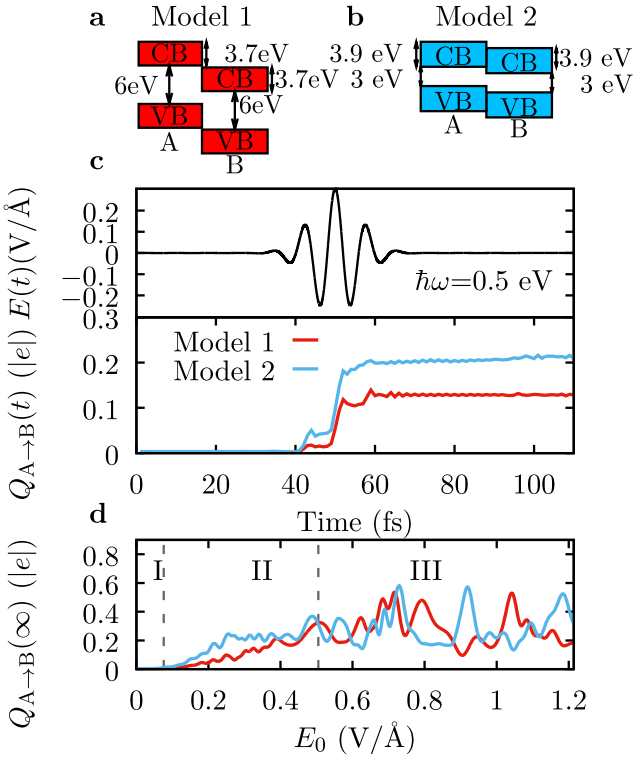

FIG. 2. Femtosecond charge transport dynamics across an insulating heterojunction induced by non-resonant few cycle laser pulses through the Stark-based scenario in Fig. 1. The scenario is tested in (**a**) a perfectly insulating heterojunction (Model 1) with no spectral overlap (tight-binding parameters $h^{\rm A}_{\rm odd}$ = 1.0 eV, $h^{\rm A}_{\rm even}$ = 7.0, $h^{\rm B}_{\rm odd}$ = −3.0 eV, $h^{\rm B}_{\rm even}$ = 3.0 eV, $t^{i}_{\rm odd} = t^{i}_{\rm even}$ = 3.0 eV, i =A,B) and (**b**) a partially insulating heterojunction (Model 2) with partial spectral overlap ($h^{\rm A}_{\rm odd}$ = 1.0 eV, $h^{\rm even}_{\rm A}$ = 4.0 eV, $h^{\rm B}_{\rm odd}$ = 0.0 eV, $h^{\rm B}_{\rm even}$ = 3.0 eV, $t^{i}_{\rm odd}$ = 2.25 eV $t^{i}_{\rm even}$ = 3.0 eV). For Model 1, these parameters yield a 3.7 eV bandwidth for each band and 6 eV bandgap; for Model 2, 3.9 eV bandwidth and 3 eV bandgap. (**c**) Charge transfer dynamics from A→B induced by the laser pulse in the top panel for both models. (**d**) Net charge transfer induced by lasers of varying amplitude E_0. Note that the effect is robust to model parameters and laser intensities.

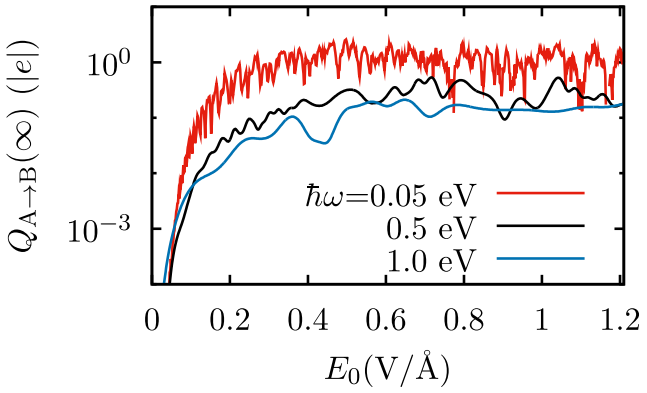

FIG. 3. Dependence of the Stark control on laser parameters for the insulating heterojunction (Model 1). The plot shows the net charge transferred using three laser pulses with different frequencies and the same number of cycles as a function of the laser amplitude. In region II (*cf.* Fig. 2), the magnitude of the effect increases with decreasing frequency.

each material. The competition between these processes leads to a complicated dependence of the effect on laser amplitude.

To further demonstrate the robustness of the control scheme on laser parameters, we quantified the net transferred charge induced by lasers with three different frequencies ($\hbar\omega = 0.05, 0.5$ and 1.0 eV) but the same number of cycles ($\tau = \sqrt{2}\pi/\omega$). As shown in Fig. 3, in the regime in which there is an appreciable effect (E_0 >0.076 V/Å), decreasing the frequency of the laser increases the amount of charge that is transferred. The reason for this is because lowering frequency increases the time in which the relevant energy levels in the two materials are near resonance, thus enhancing the effectiveness of the tunneling mechanism.

Figures 4a-b illustrate the dependence of the effect on the strength of the interfacial tight-binding coupling $t_{\rm AB}$ (with $\hbar\omega = 0.5$ eV). As shown, increasing $t_{\rm AB}$ monotonically increases the magnitude of the effect for all laser amplitudes considered, as it enhances the tunneling probability across the interface. Figure 4c shows the dependence of the effect on the interfacial distance $a_{\rm AB}$ for fixed interfacial tight-binding coupling [$t_{\rm AB}$ = 0.2 eV, $E_0 = 0.3$ V/Å ($I_0 = 1.2\times10^{12}$ W/cm^2), $\hbar\omega$ =0.5 eV]. As shown, the amount of charge that is transferred generally increases as the interfacial distance increases. To understand this, consider a minimal single band model per material in the heterojunction. In the presence of a strong electric field, the energy eigenstates transition from delocalized states to localized Wannier-Stark (WS) states. The energy of the WS state localized at site m of material i =A,B with position x_m is given by $\varepsilon^i_m \cong \varepsilon^i_0 + x_m|e|E$, where ε^i_0 is the energetic center of the band. The electric field at which there is a crossing between a level localized at site m of A and site n of B is $E = \frac{\varepsilon^{\rm A}_0 - \varepsilon^{\rm B}_0}{x_m - x_n}$. As $a_{\rm AB}$ increases, $x_m - x_n$ increases leading to a decrease in the E required to induce the crossing. Thus, increasing $a_{\rm AB}$ generally increases the charge transfer because the same laser pulse can induce more crossings contributing to the effect.

To test the effectiveness of the scenario in a heterojunction with partial spectral overlap, we quantified the control in a second model, in which both the VBs and CBs of the two materials overlap by 2.9 eV (Model 2, Fig. 2b). As shown in Fig. 2, the scenario is also robust in this model. With respect to Model 1, the reduced 3 eV bandgap of Model 2 leads to an effect with larger magnitude for $E_0 \leq$0.4 V/Å ($I_0 \leq 2.1\times10^{12}$ W/cm^2) and a reduction in the range of electric field amplitudes for which A→B interband tunneling dominates the dynamics. In fact, for $E_0 \gtrsim 0.25$ V/Å ($I_0 \gtrsim 8.3\times10^{11}$ W/cm^2) the laser pulse is intense enough to induce crossings be-

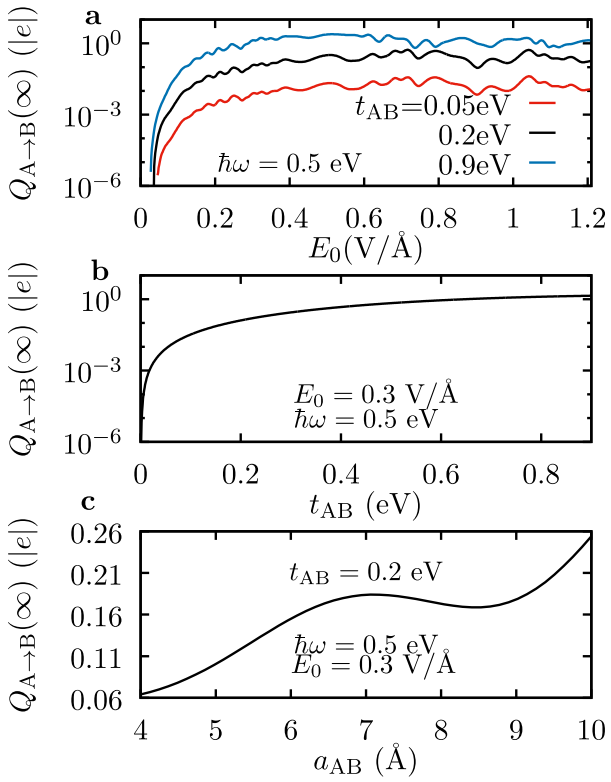

FIG. 4. Dependence of the Stark control on the interfacial parameters. (**a**,**b**) Influence of the interfacial tight-binding coupling t_{AB} on the magnitude of the effect for different laser amplitudes. (**c**) Impact of the interfacial distance a_{AB} for a fixed interfacial coupling t_{AB} =0.2 eV.

tween the VB of B and the CB of A that leads to B→A charge transfer and a complicated dependence of the effect on laser amplitude.

To demonstrate that quantum tunneling dominates the dynamics in the computational observations, we model the dynamics using a rate equation with transition probabilities determined by Landau-Zener (LZ) theory[34,35]. We focus on Region II of Model 1 (Fig. 2d) where only the VB of material A and the CB of B play a prominent role in the photoinduced process. We thus consider a minimal model in which the single-particle states in the VB of A and the CB of B are the only states allowed to exchange charge from time t to time $t+\Delta t$ as

$$\eta_l^{\rm B}(t+\Delta t) = \eta_l^{\rm B}(t) + (\eta_k^{\rm A}(t) - \eta_l^{\rm B}(t))P_{k{\rm A}\to l{\rm B}}(t), \quad (3)$$

where η_l^α is the population of the lth level of material α =A or B, and $P_{k{\rm A}\to l{\rm B}}(t) = P_{l{\rm B}\to k{\rm A}}(t)$ is the LZ tunneling probability

$$P_{k{\rm A}\to l{\rm B}}(t_{\rm crossing}) = 1 - e^{-\beta_{l{\rm B}}^{k{\rm A}}}, \quad (4)$$

with

$$\beta_{l{\rm B}}^{k{\rm A}} = \frac{2\pi(\Delta_{l{\rm B}}^{k{\rm A}})^2}{\hbar|d/dt(\varepsilon_k^{\rm A}(E(t)) - \varepsilon_l^{\rm B}(E(t)))|_{t=t_{\rm crossing}}}, \quad (5)$$

at the crossing time, and zero otherwise. Here $\Delta_{l{\rm B}}^{k{\rm A}}$ is the energy gap between the kth VB level of A and the lth CB level of B at the avoided crossing, and ε_l^i the energies of the associated diabatic states. For strong laser fields, the Stark shifted energies vary linearly with the electric field such that $\frac{d\varepsilon_l^i}{dt} = M_l^i \frac{dE(t)}{dt}$. In calculating Eq. (3), the slopes M_l^i are determined by linear regression around the relevant avoided crossing.

Figure 5 compares the charge transfer dynamics obtained by the LZ rate equation with that from the time-dependent Schrödinger equation for two laser frequencies ($\hbar\omega$ = 0.05 and 0.5 eV), and maximum field amplitude E_0 =0.21 V/Å. In both cases the rate equation based on LZ tunneling reproduces the qualitative features of the charge transfer dynamics obtained through quantum dynamics. Note that LZ rate equation reproduces quantitatively the simulated charge transfer rate for all transitions except the ones around $t\omega/2\pi \approx 1.0$ which it overestimates. The overestimation arises because LZ theory requires the diabatic energies to change linearly with time [36] in the crossing region, and that condition is not satisfied around $t\omega/2\pi \approx 1.0$ where the electric field of light is near a maximum. When the variation of the oscillating electric field of the laser can be well approximated by a linear function of time in the crossing, the LZ rate equation quantitatively reproduces the dynamics. These results indicate that the charge transfer is due to interband LZ quantum tunneling across the interface induced by Stark shifts.

To demonstrate that the scenario survives even in the presence of decoherence, we repeated the LZ rate computations but with the modified transition probability, $P_{k{\rm A}\to l{\rm B}}^{\rm incoh}(t_{\rm crossing}) = (1 - e^{-2\beta_{l{\rm B}}^{k{\rm A}}})/2$, that has been isolated for the LZ process in the presence of strong decoherence[37–39]. As can be seen in Fig. 5 (black dashed lines), the decoherence has a very mild influence in the scenario for the two laser frequencies considered because the control is in the regime in which $\beta_{l{\rm B}}^{k{\rm A}}$ is small for most crossings where $P_{k{\rm A}\to l{\rm B}}^{\rm incoh}$ numerically coincides with that in Eq. (4).

In conclusion, we have introduced a novel Stark-based laser control scenario to manipulate electronic dynamics at material interfaces. The scenario is based on using non-resonant light of intermediate intensity to create transient resonances between conduction and valence band levels of two different adjacent materials, that open tunneling channels for electron transport across their interface. The scenario was employed to transiently transform an insulating heterojunction into a conducting one on a femtosecond timescale. Quantum dynamics simulations demonstrate that in the regime where Stark effects dominate the dynamics, the effect is robust to changes in the laser frequency and amplitude. The scheme can be employed for the development of ultrafast electronics and optical actuators.

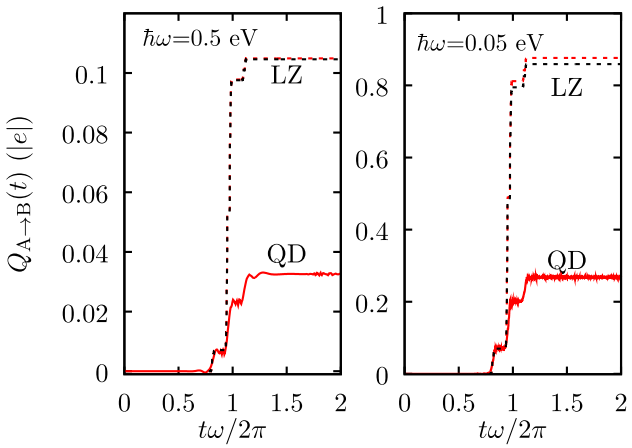

FIG. 5. Comparison of Landau-Zener rate theory (red dashed lines) with the full quantum dynamics (red solid lines), and effect of decoherence. The plots show the A→B transferred charge induced by the laser (E_0 =0.21 V/Å) for two central frequencies ($\hbar\omega$ = 0.05 and 0.5 eV). Note the LZ rate equations reproduce the basic features of the quantum dynamics, indicating that the effect is due to quantum tunneling processes induced by Stark shifts. Introducing decoherence to the LZ rate equations (black dashed lines) has a minor effect on the dynamics.

ACKNOWLEDGMENTS

This material is based on the work supported by the National Science Foundation under No. CHE-1553939.

* ignacio.franco@rochester.edu

[1] M. Shapiro and P. Brumer, *Quantum Control of Molecular Processes*, 2nd ed. (Wiley-VCH, Weinheim, 2012).
[2] S. A. Rice and M. Zhao, *Optical control of molecular dynamics* (John Wiley & Sons, New York, 2000).
[3] F. Krausz and M. Ivanov, Rev. Mod. Phys. **81**, 163 (2009).
[4] G. Fleming and M. Ratner, Physics Today **61**, 28 (2008).
[5] T. L. Cocker, D. Peller, P. Yu, J. Repp, and R. Huber, Nature **539**, 263 (2016).
[6] V. Jelic, K. Iwaszczuk, P. H. Nguyen, C. Rathje, G. J. Hornig, H. M. Sharum, J. R. Hoffman, M. R. Freeman, and F. A. Hegmann, Nat. Phys. **13**, 591 (2017).
[7] T. Rybka, M. Ludwig, M. F. Schmalz, V. Knittel, D. Brida, and A. Leitenstorfer, Nat. Photonics **10**, 667 (2016).
[8] T. Higuchi, C. Heide, K. Ullmann, H. B. Weber, and P. Hommelhoff, Nature **550**, 224 (2017).
[9] A. Schiffrin, T. Paasch-Colberg, N. Karpowicz, V. Apalkov, D. Gerster, S. Mühlbrandt, M. Korbman, J. Reichert, M. Schultze, S. Holzner, J. V. Barth, R. Kienberger, R. Ernstorfer, V. S. Yakovlev, M. I. Stockman, and F. Krausz, Nature **493**, 70 (2013).
[10] M. Schultze, E. M. Bothschafter, A. Sommer, S. Holzner, W. Schweinberger, M. Fiess, M. Hofstetter, R. Kienberger, V. Apalkov, V. S. Yakovlev, M. I. Stockman, and F. Krausz, Nature **493**, 75 (2013).
[11] I. Franco, M. Shapiro, and P. Brumer, Phys. Rev. Lett. **99**, 126802 (2007).
[12] J. G. Underwood, M. Spanner, M. Y. Ivanov, J. Mottershead, B. J. Sussman, and A. Stolow, Phys. Rev. Lett. **90**, 223001 (2003).
[13] B. J. Sussman, D. Townsend, M. Y. Ivanov, and A. Stolow, Science **314**, 278 (2006).
[14] L. Chen, Y. Zhang, G. H. Chen, and I. Franco, Nature Comm. **9**, 2070 (2018).
[15] M. E. Corrales, R. de Nalda, and L. Bañares, Nat. Commun. **8**, 1345 (2017).
[16] I. R. Solá, B. Y. Chang, J. Santamaría, V. S. Malinovsky, and J. L. Krause, Phys. Rev. Lett. **85**, 4241 (2000).
[17] H. Niikura, P. B. Corkum, and D. M. Villeneuve, Phys. Rev. Lett. **90**, 203601 (2003).
[18] E. J. Sie, J. W. McIver, Y.-H. Lee, L. Fu, J. Kong, and N. Gedik, Nat. Mater. **14**, 290 (2014).
[19] I. Franco, M. Shapiro, and P. Brumer, J. Chem. Phys. **128**, 244906 (2008).
[20] A. Kar and I. Franco, J. Chem. Phys. **146**, 214107 (2017).
[21] B. Gu and I. Franco, J. Phys. Chem. Lett. **8**, 4289 (2017).
[22] B. Gu and I. Franco, J. Phys. Chem. Lett. **9**, 773 (2018).
[23] W. Hu, B. Gu, and I. Franco, J. Chem. Phys. **148**, 134304 (2018).
[24] V. E. V.M. Galitskii, S.P. Goreslavskii, JETP **30**, 117 (1970).
[25] T. Oka and H. Aoki, Phys. Rev. B **79**, 081406 (2009).
[26] N. H. Lindner, G. Refael, and V. Galitski, Nature Physics **7**, 490 (2011).
[27] Y. H. Wang, H. Steinberg, P. Jarillo-Herrero, and N. Gedik, Science **342**, 453 (2013).
[28] S. V. Syzranov, Y. I. Rodionov, K. I. Kugel, and F. Nori, Phys. Rev. B **88**, 241112 (2013).
[29] B. Gu and I. Franco, ArXiv e-prints (2018), arXiv:1806.09217.
[30] M. Lenzner, J. Krüger, S. Sartania, Z. Cheng, C. Spielmann, G. Mourou, W. Kautek, and F. Krausz, Phys. Rev. Lett. **80**, 4076 (1998).
[31] O. Schubert, M. Hohenleutner, F. Langer, B. Urbanek,

C. Lange, U. Huttner, D. Golde, T. Meier, M. Kira, S. W. Koch, and R. Huber, Nat. Photonics **8**, 119 (2014).
[32] A. C. Hindmarsh, P. N. Brown, K. E. Grant, S. L. Lee, R. Serban, D. E. Shumaker, and C. S. Woodward, ACM Transactions on Mathematical Software (TOMS) **31**, 363 (2005).
[33] C. Zener, Proc. Royal Soc. Lond. **145**, 523 (1934).
[34] C. Zener, Proc. Royal Soc. Lond. **137**, 696 (1932).
[35] L. D. Landau, Phys. Z. Sowjetunion **2**, 43 (1932).
[36] J. R. Rubbmark, M. M. Kash, M. G. Littman, and D. Kleppner, Phys. Rev. A **23**, 3107 (1981).
[37] Y. Kayanuma, J. Phys. Soc. Jpn. **53**, 108 (1984).
[38] Y. Kayanuma, J. Phys. Soc. Jpn. **54**, 2037 (1985).
[39] P. Ao and J. Rammer, Phys. Rev. Lett. **62**, 3004 (1989).